

# Numerical Simulation of Vortex Combustion in a Hybrid Rocket Motor

Jakub Glowacki\*<sup>†</sup>, Filippo Maggi\* and Luciano Galfetti\*

\*Politecnico di Milano

Milan, Italy

jakub.glowacki@polimi.it · filippo.maggi@polimi.it · luciano.galfetti@polimi.it

<sup>†</sup>Corresponding author

## Abstract

The main aim of the article is to investigate the vortex pancake hybrid motor (VPH), which is being considered to be a perspective solution for future small thrusters based on hybrid technology. Developed numerical simulation solves Navier-Stokes equations taking into account complex multi-step chemical kinetics, radiation and solid-fluid interaction occurring on the surface of the fuel grain. The closure of the analytical model is obtained with a use of Large Eddy Simulation (LES) for turbulence, Partially Stirred Reactor (PaSR) and Discrete Ordinates Method (DOM) for radiation. The model was evaluated and verified based on experimental and literature results in 2D slab configuration. Then it is applied for VPH configuration giving the flow pattern and the distribution of the reacting species. Parametric studies shows the most favorable configuration and estimates main fuel release zones giving indications for the design of future hybrid pancake engines.

## 1. Introduction

Hybrid rocket engines (HREs) has been considered as one of the most perspective alternatives for solid and liquid propulsion systems for over 50 years. However, well defined problems such as low regression rate  $r_f$  of the solid fuel and poor combustion efficiency, which limit its applicability have never been solved. Nevertheless, recent international efforts, in investigating space launchers suggest that HREs experience its renaissance.<sup>3</sup> The technology offers high performance (in terms of specific impulse  $I_s$ ) combined with safety, operating flexibility and cost reduction. On the side of the mainstream of interested stays the application of HREs for in-space missions (as de-orbiting, soft landing, orbit transfers, attitude control and propulsion for micro satellites). This specific field of space exploration has been often associated with HREs due its throteability and re-ignition capability but it has never been carefully investigated. Current methods of approaching limitations of HREs diverge in between modification of fuel composition and gas flow alteration. The second method is technically realized by vortex flow or swirling jets<sup>26</sup> and is inherently connected with the change in a oxidizer injector design. It had been observed that although swirl flow proves to increase regression rate in laboratory scale motor the results are not scalable for full-scale motors due to the viscous damping of the tangential component of oxidizer velocity.<sup>2</sup> This however, is not a limitation for small thrusters for in-space maneuvering. A comprehensive investigation of technical implementation of the flow enhancement for small HREs was done by Haag et al. at the Surrey Space Center<sup>1415</sup> and revealed a high potential of vortex pancake hybrid (VPH) configuration. The fundamental difference in respect to hybrids in classic configuration is that the VPH engine has the flat cylindrical fuel, without the channel located along the axis of symmetry, and the oxidizer is injected perpendicular to the fuel grain and to the exit port (Fig. 1).

Previous research on VPHs showed that the engine in this configuration can mitigate several disadvantages of HREs. It does not experience typical for HREs oxidizer-to-fuel ratio shifts, has a high combustion efficiency (up to 99%<sup>9</sup>) and the optimal length-to-diameter ratio  $<1^{18}$  which makes it a compact design for small satellites missions. Pioneering work in this field done by Haag et al.<sup>1415</sup> was an experimental investigation, with parametric studies of various physical (pressure, injection velocity, oxidizer mass flow rate) and chamber design parameters (number of injectors, fuel grain diameter). Further research performed by Rice et al.<sup>10</sup> however put several previously obtained results in question, they were very often contradictory to the one from the work of Haag. Therefore the dependency of the chamber height, mass flow rate, pressure effects, scalability on system performance were not conclusive. Recent reinvestigation of VPH done by Paravan et al.<sup>5</sup> had taken more comprehensive form. Experimental investigation was

## NUMERICAL SIMULATION OF VORTEX COMBUSTION IN A HYBRID ROCKET MOTOR



Figure 1: Vortex flow pancake hybrid rocket engine

aided with CFD modeling to understand flow patterning in the combustion chamber. Performed cold flow simulations investigated the combustion chamber optimal height, visualizing the flow pattern for different oxidizer velocities.

### 1.1 Hybrid Rocket Engine combustion modeling - literature review

The combustion mechanism in a HRE is a complex process which involves chemical reactions, heat transfer coupled with turbulent flow dynamics. All reactions in between species take place inside the boundary layer which is formed above the surface of the fuel. The combustion is fed by the fuel pyrolysis gases, which are released according to the surface temperature of the grain. The temperature pick is located in front of the grain and decreases along the grain length. The intensity of the combustion depends on the amount of fuel gases that are transferred to the reaction zone by convection and diffusion. The energy than is transferred back to the fuel mostly by conduction, radiation and convection. The convection is partially limited by the pyrolysis gases which are ejected from the fuel surface and the phenomena known as the *blocking effect*.

Existing mathematical models used to analyze the hybrid rocket combustion and solid fuel behavior are based on the work of Marxman et al.<sup>20,21</sup> who derived the theoretical treatment of the hybrid rocket combustion in 1963. Marxman and co-workers correctly identified most of the parameters that influence the hybrid rocket motor combustion. Their model was based on the assumption of diffusion flame in the boundary layer over the fuel surface. The heat transfer was modeled using both convection and conduction, with limited attention to the radiation. For the regression rate modeling Marxman proposed an regression rate model based on the equation  $\dot{r} = a \cdot G_{ox}^n$ . Despite of many attempts to correlate the result with various combustion chamber thermodynamical parameters done in 60' by Smoot et al<sup>22</sup> the model of Marxman stays a dominant one for HRE combustion modeling.

Full analytical description of the problem is described by 4 coupled partial differential equations which cannot be solved analytically in their most general form. The solution came with the development of computational power and spread of computational fluid dynamic techniques. In 1994 Cheng et al.<sup>11</sup> made a full 3D simulation for the DM-1 AMROC engine obtaining realistic and verifiable results with a use of  $k-\varepsilon$  RANS model and simple chemical kinetics. Another approach proposed by Lin et al.<sup>7</sup> modeled oxidizer flow and the combustion with Eulerian-Eulerian spray. This allowed the parametric studies of the oxidizer inflow condition and its influence on the combustion efficiency. Scaling problem of HREs was investigated by Sankar et al.<sup>24</sup> who developed the model for slab burner and compared the results for different engine sizes. He proved that CFD methods can give a valuable asset in finding solution to the problem.

Those early works were later followed by several other publications that were investigating influences of different physical parameters. Serin et al.<sup>25</sup> used a commercial software for the investigation of the slab burner flow field. The pressure dependency, which has been argued since the times of the first Marxman models, has been also investigated using CFD models by Gariani et al.<sup>13,12</sup> and Coronetti et al.<sup>8</sup> both performed their simulations using open-source

## NUMERICAL SIMULATION OF VORTEX COMBUSTION IN A HYBRID ROCKET MOTOR

OpenFoam framework<sup>17</sup> and were verified by the sets of burning tests. Gariani also developed the model to simulate the influence of the high-energy additives on flow field characteristics. Finally, the swirling flow has been numerically modeled by Knuth<sup>19</sup> aiding the experimental results that proved that the concept has a significant influence on both - combustion efficiency and the regression rate.

## 2. Analytical Model

To find the analytical solution of the flow field inside the combustion chamber of a HRE the analytical model was formulated by means of the flow governing equations, chemical kinetics and solid-fluid interaction. The major role plays the choice of the turbulence model, due to its interaction with the chemical kinetics.

### 2.1 Governing Equations

With the assumption of the Newtonian fluid the governing equations inside the combustion chamber is modeled by 4 main equations:

- Continuity equation

$$\frac{\partial \bar{\rho}}{\partial t} + \frac{\partial \bar{\rho} \bar{u}_j}{\partial x_j} = 0 \quad (1)$$

- Momentum conservation equation

$$\frac{\partial \bar{\rho} \bar{u}_i}{\partial t} + \frac{\partial \bar{\rho} \bar{u}_i \bar{u}_j}{\partial x_j} = -\frac{\partial \bar{p}}{\partial x_i} + \frac{\partial \bar{\tau}_{ij}}{\partial x_j} - \frac{\partial \overline{\rho u'_i u'_j}}{\partial x_j} \quad (2)$$

- Energy conservation equation

$$\frac{\partial \bar{\rho} \bar{h}_t}{\partial t} + \frac{\partial \bar{\rho} \bar{h}_t \bar{u}_j}{\partial x_j} = \frac{\partial \bar{p}}{\partial t} + \frac{\partial}{\partial x_j} (-\bar{\rho} \alpha \frac{\partial \bar{h}}{\partial x_j} + \bar{u}_i \bar{\tau}_{ij}) + \bar{Q}_{rad} + \sum_{k=1}^N \bar{\rho} h_f \bar{\omega}_k - \frac{\partial \overline{\rho h'_t u'_j}}{\partial x_j} \quad (3)$$

- Species conservation equation

$$\frac{\partial \bar{\rho} \bar{Y}_k}{\partial t} + \frac{\partial \bar{\rho} \bar{Y}_k \bar{u}_j}{\partial x_j} = \frac{\partial}{\partial x_i} (\bar{\rho} D_k \frac{\partial \bar{Y}_k}{\partial x_i}) + \bar{\omega}_k - \frac{\partial \overline{\rho Y'_k u'_j}}{\partial x_j} \quad (4)$$

Additionally the model of solid-fluid interaction requires two additional relations to be solved. The model is expressed by two equation:

- Continuity equation

$$\frac{\partial \rho_f}{\partial t} + \frac{\partial \rho_f u_f}{\partial x} = 0 \quad (5)$$

- Energy conservation equation

$$\frac{\partial \rho_f h_f}{\partial t} = \frac{d}{dx} \lambda \frac{dT}{dx} + \dot{m}_{(g)} h_g(T) + \vec{q}_{rad} + \dot{\omega} \quad (6)$$

### 2.2 Turbulence, radiation and chemical kinetics closure model

The Reynolds averaging procedure used in the description of the equations 2 - 4 introduced additional terms - Reynolds stresses, turbulent thermal flux and mass diffusion which are responsible for the turbulence and require three additional definitions:

- The first equation needed to completely define the solution is a turbulent transport of mass in general form defined as:

$$\overline{\rho u'_j Y'_k} = -\frac{\mu_T}{Pr_T Le_T} \frac{\partial \bar{Y}_k}{\partial x_j} \quad (7)$$

where  $Pr = \frac{\nu}{\alpha}$ ,  $Le = \frac{\alpha}{D}$  are the Prandtl and Lewis numbers.

## NUMERICAL SIMULATION OF VORTEX COMBUSTION IN A HYBRID ROCKET MOTOR

- The Reynolds stress tensor,  $\tau_{ij}^R = \overline{\rho u'_i u'_j}$ , under Boussinesq hypothesis, can be defined as:

$$\tau_{ij}^R = \mu_T \left( \frac{\partial U_i}{\partial x_j} - \frac{\partial U_j}{\partial x_i} \right) - \frac{2}{3} \bar{\rho} k \delta_{ij} \quad (8)$$

where the turbulent kinetic energy is defined as:

$$k = \frac{1}{2} \overline{u'_i u'_i} \quad (9)$$

- The last unknown part of the solution is the turbulent transport of energy which can be expressed as

$$\overline{\rho u'_j h'_i} = - \frac{\mu_T}{Pr_T Le_T} \frac{\partial \bar{Y}_k}{\partial x_j} \bar{h}_i - \frac{\mu_T}{Pr_T} \frac{\partial \bar{h}_i}{\partial x_j} + \left( \mu + \frac{\mu_T}{\sigma_k} \right) \frac{\partial k}{\partial x_j} \quad (10)$$

Chemical source term  $\bar{\omega}$  is the component responsible for the energy coming from chemical reactions and is included in the relations 3 and 6. Chosen approach, already introduced in the work of Mazzetti<sup>4</sup> is to model the closure by the Partially Stirred Reactor (PaSR).<sup>23</sup> The reacting part is modeled as a perfectly stirred reactor (PSR) with the three characteristic times: a chemical time  $\tau_c$ , a turbulent mixing time  $\tau_{mix}$  and a residence time  $\delta\tau$ . Those parameters are linked together with the reaction rate factor  $\kappa$

$$\kappa = \frac{\delta\tau + \tau_c}{\delta\tau + \tau_c + \tau_{mix}} \quad (11)$$

which, along with the reaction rate  $R_k$  defines the chemical source term

$$\bar{\omega} = \kappa R_k \quad (12)$$

The reaction rate of the species k is defined as follows

$$R_k = \sum_{j=1}^{N_R} (v''_{kj} - v'_{kj}) R_j \quad (13)$$

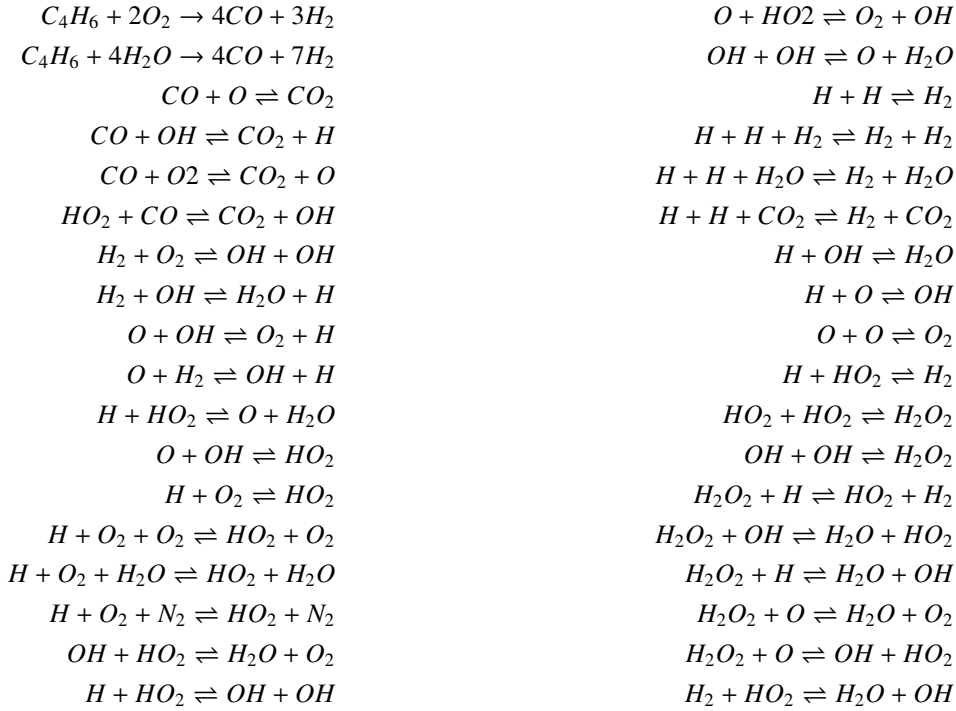
where  $v''_{kj}$  and  $v'_{kj}$  are stoichiometric coefficients of species k in the reaction j.  $R_j$  can be obtained from the Arrhenius law which is a non-linear function of mixture temperature described as

$$R_j = A T^b \exp\left(-\frac{E_a}{RT}\right) \prod_{k=1}^{N_r} (C_{Mk})^{v'_k} \quad (14)$$

where  $E_a$  is the activation energy,  $N_r$  the number of reactants, A the pre-exponentiation coefficient, b the temperature exponent.

The fuel-oxidizer couple chosen for the simulation is hydroxyl-terminated polybutadiene (HTPB) with oxygen. As reported by Risha et al.<sup>16</sup> the main gaseous component in high temperature pyrolysis of HTPB is Butadiene  $C_4H_6$  whose mole fraction at the temperature of 1073 K is twice times higher compared to the second component of the pyrolysis Benzen  $C_6H_6$ . Other products like Propene ( $C_3H_6$ ), Toluene ( $C_7H_6$ ) and 3-Peten-1-Yene ( $C_5H_6$ ) are even less prominent thus it is justified to consider the butadine as the only product of the solid fuel decomposition. The main gaseous products of the reaction in between HTPB and  $O_2$  are  $CO_2$  and  $H_2O$ . From those, further decomposition of  $H_2O$  plays a significant role due to its endothermic nature, by which it controls the process affecting the combustion temperature. Therefore, in this work the detailed chemical scheme with 36 reaction involving 13 species was proposed with the particular attention to model  $H_2O$  decomposition.

## NUMERICAL SIMULATION OF VORTEX COMBUSTION IN A HYBRID ROCKET MOTOR



The radiation contribution to the equation 3 was obtained using Discrete Ordinates Method closure. To analyze the problem of heat transfer propagating in the given direction  $\vec{s}$ , through a unit area normal to  $\vec{s}$  the radiation equation can be written as

$$\frac{dI(\vec{s})}{dl} = -(k + \sigma_s)I(\vec{s}) + kI_b + \frac{\sigma_s}{4\pi} \int_{4\pi} I(\vec{s}')\Psi(\vec{s}', \vec{s})d\Omega' \quad (15)$$

where  $I(\vec{s})$  is the radiation intensity in the direction  $\vec{s}$ ,  $k$  the absorption coefficient,  $l$  the length parameter along direction  $\vec{s}$ ,  $\sigma_s$  the scattering coefficient,  $\Psi(\vec{s}', \vec{s})$  the phase scattering function. DOM treats the integral term of the equation 15 by means of a Gaussian quadrature over the solid angle.

$$\int_{4\pi} I(\vec{s}')\Psi(\vec{s}', \vec{s})d\Omega' \approx \sum_{k=1}^N \omega_k I^k(\vec{s}')\Psi(\vec{s}', \vec{s}) \quad (16)$$

### 3. 2-Dimension Benchmark Case

The simulation performed on the benchmark case has two main objectives: compare the results using different methodology and to verify the tool so it could be applied to simulate more sophisticated 3 dimensional problems. The solution to the numerical model was obtained employing Finite Volume Method within OpenFoam<sup>117</sup> framework .

Table 1: Benchmark case boundary conditions

Patch Name	$p$ [Pa]	$T$ [K]	$U$ [m/s]	$k$ [ $\frac{m^2}{s^2}$ ]
Inlet	$\frac{\partial p}{\partial x} = 0$	TV <sup>a</sup>	6, 12, 17, 20	0.001
Outlet	$10^5$	$\frac{\partial T}{\partial x} = 0$	$\frac{\partial \vec{U}}{\partial x} = 0$	$\frac{\partial k}{\partial x} = 0$
Bottom Wall	$\frac{\partial p}{\partial y} = 0$	$\frac{\partial T}{\partial y} = 0$	$\vec{U} = 0$	$\frac{\partial k}{\partial y} = 0$
Top Patch	Symmetry	Symmetry	Symmetry	Symmetry
Fuel Patch	-	300	-	-

<sup>a</sup>Time Variant

The geometry for the benchmark case simulation represented 2 dimensional slab. The computational domain consists of two different domains coupled with the interaction boundary condition. In the fluid domain the full set of

## NUMERICAL SIMULATION OF VORTEX COMBUSTION IN A HYBRID ROCKET MOTOR

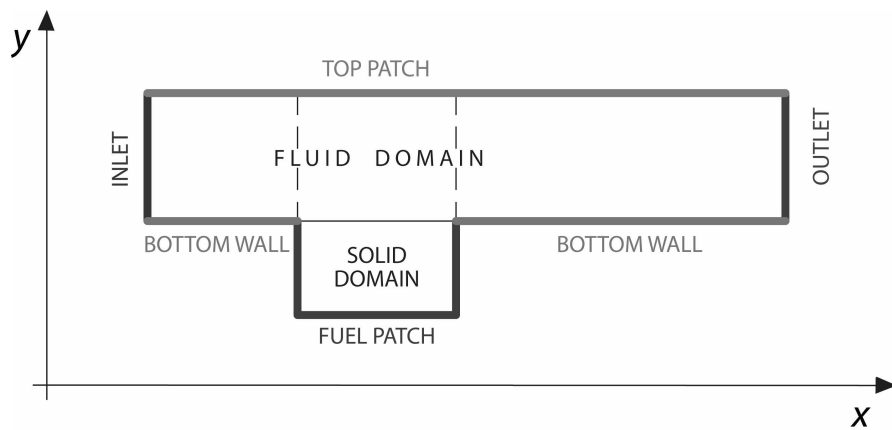
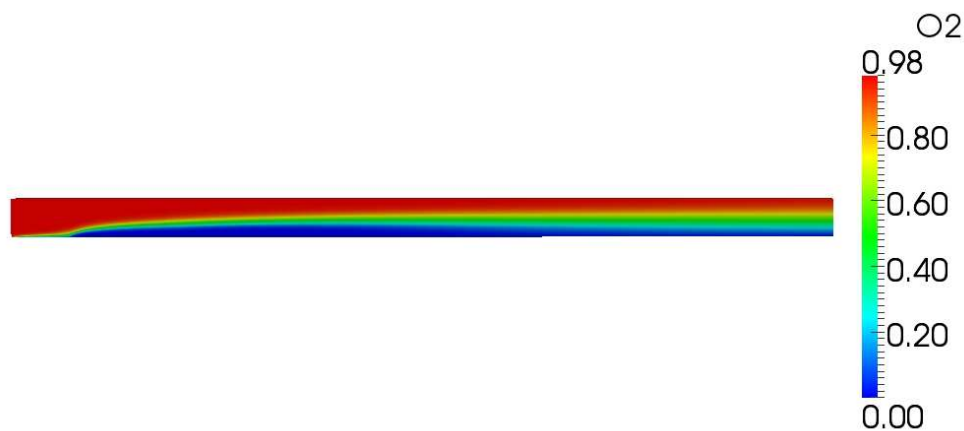


Figure 2: Benchmark case boundary conditions

equations, introduced in the previous section, is solved while in the solid domain only conduction equation is calculated (ref. Fig. 2).



Figure 3: Temperature flow field [K]

Figure 4:  $O_2$  mass fraction

The geometry chosen for this analysis is based on the previous investigation done by Gariani et al.<sup>12</sup> and Coronetti.<sup>8</sup> Both investigated the case which is 0.05 m in length and 0.002 m in high. The length of the pre-combustion chamber was chosen to be 0.03 m while the post-combustion 0.4 m. The results from the figures 3 -4 and the one

## NUMERICAL SIMULATION OF VORTEX COMBUSTION IN A HYBRID ROCKET MOTOR

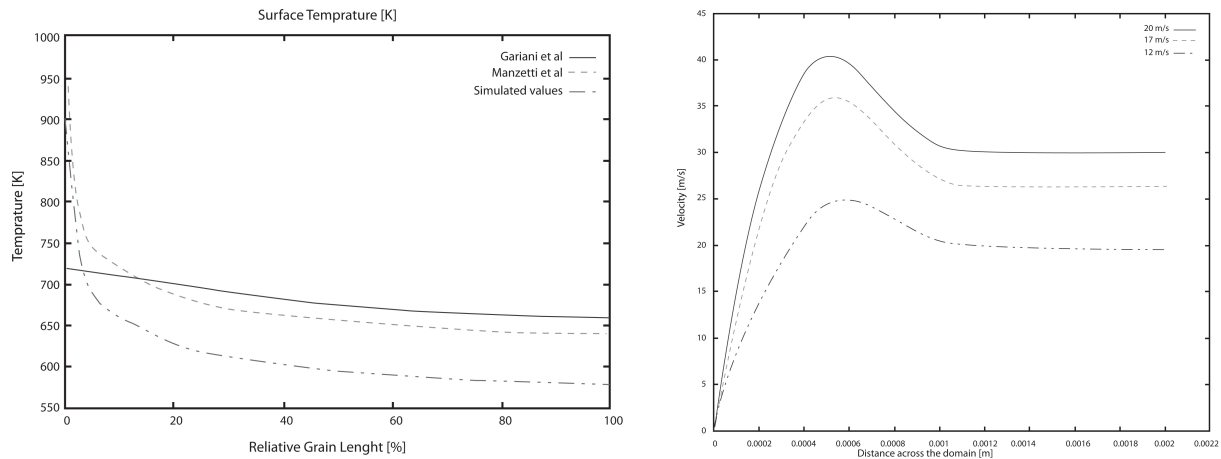


Figure 5: Surface temperature comparison in respect to the different computation models

Figure 6: Inlet Velocity influence on the velocity across the domain

obtained from the literature shows the mixing length of the diffusive flame which justify the choice of the long post-combustion chamber. The temperature profile on the solid fuel surface (ref. Fig. 5) which guides the regression rate is coherent with results obtained from the literature. Also the parametric analysis of different oxidizer inlet velocities shows correctly its influence on the flame height.

#### 4. Pancake Hybrid Rocket Cold Flow Simulation

The numerical model, which validity was confirmed in the previous section was introduced to find the flow pattern in VPH. Firstly the analysis was based on the assumption of the cold flow - with the chemical reactions in between species neglected. The geometry was coherent with the one proposed by Haag et al.<sup>15</sup> and is presented in the table 2 while the imposed boundary conditions are presented in 3. In the evaluated model the fuel was located only on the bottom side of the case. There was also no central perforation, to evaluate the amount of fuel gases released and the central fuel patterning reported by Rice<sup>10</sup> and connected by Chiaverini with the *recirculation effect*.<sup>6</sup>

Table 2: VPH model specification

Parameter	Comment
Case diameter	120 mm
Case high	11 mm
Number of injectors	1,2 and 4
Inert species	$CO_2$
Oxidizer	Air
Oxidizer inlet velocity	10 [m/s]
Pressure	$10^6 [Pa]$
Fuel	Methane $CH_4$

Table 3: Cold Flow Boundary Conditions

Patch Name	$p$ [Pa]	$T$ [K]	$U$ [m/s]	$k$ [ $\frac{m^2}{s^2}$ ]
Inlet	$\frac{\partial p}{\partial x} = 0$	300	$10 \cdot \vec{n}$	0.958
Outlet	$10^6$	$\frac{\partial T}{\partial y} = 0$	$\frac{\partial \vec{U}}{\partial y} = 0$	$\frac{\partial k}{\partial y} = 0$
External Walls	$\frac{\partial p}{\partial x} = 0$	$\frac{\partial T}{\partial x} = 0$	$\vec{U} = 0$	$\frac{\partial k}{\partial x} = 0$
Fuel	$\frac{\partial p}{\partial y} = 0$	$\frac{\partial T}{\partial y} = 0$	$0.1 \cdot \vec{n}$	$\frac{\partial k}{\partial y} = 0$

Due to the fact that reaction rate controls the release of the fuel gases from the fuel surface; the intensity of the process can be evaluated by computing spatial distribution of the oxidizer and fuel gases using cold flow model. More uniform distribution of the oxidizer should lead to the more uniformly distributed fuel liberation zones. This in turn should lead to the higher performance of the engine.

Simulation without reactions involved, lead to the results which expose the oxidizer-fuel mixing pattern. As it is visible on the figures 7 - 16 the amount of oxidizers inlets influences the oxidizer distribution across the combustion chamber. Moreover, the oxidizer jets cross-influence attributes to the longer fuel exposure time which leads to the higher combustion efficiency. The oxidizer deflection also ensure the additional oxidizer presence in the peripheral areas increasing combustion efficiency. The cold flow studies suggest that the combustion will take place on the sides of the oxidizer jets in the vicinity of the injector, causing high heat release in corresponding fuel areas. The location of the fuel release regions might be deduced from the oxidizer/fuel mixture ratio. This conclusion converge with the experimental work and indications for the literature<sup>15,10,5</sup> which showed that the fuel release zones were on the

## NUMERICAL SIMULATION OF VORTEX COMBUSTION IN A HYBRID ROCKET MOTOR

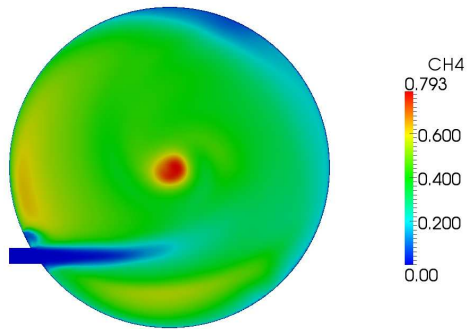


Figure 7: Fuel gases flow field for 1 inlet configuration

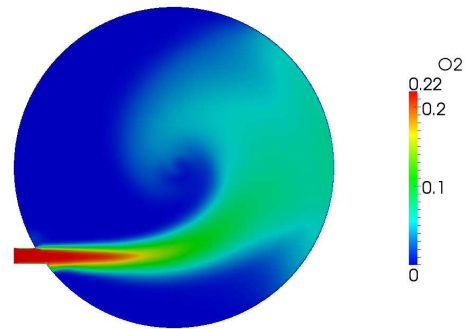


Figure 8: Oxygen flow field for 1 inlet configuration

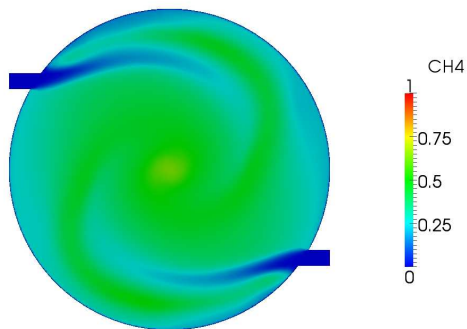


Figure 9: Fuel gases flow field for 2 inlet configuration

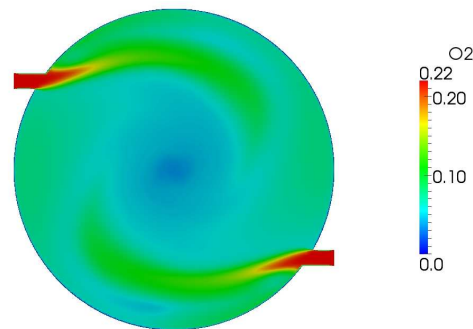


Figure 10: Oxygen flow field for 2 inlet configuration

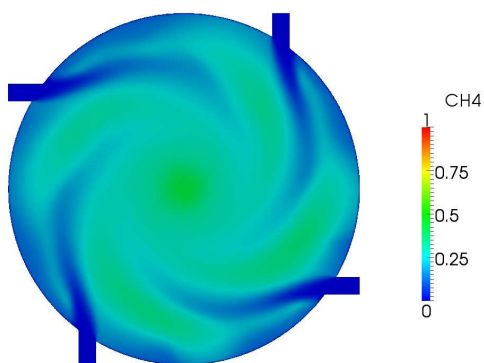


Figure 11: Fuel gases flow field for 4 inlets configuration

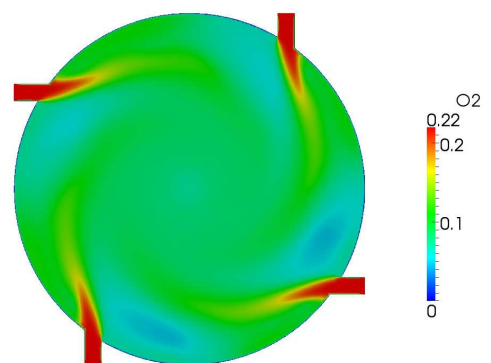


Figure 12: Oxygen flow field for 4 inlets configuration

peripheral areas and in the center of the disk. Furthermore, there is an evidence that the fuel gases are concentrated in the center of the grain due to the momentum transfer from the upcoming oxidizer stream.

## NUMERICAL SIMULATION OF VORTEX COMBUSTION IN A HYBRID ROCKET MOTOR

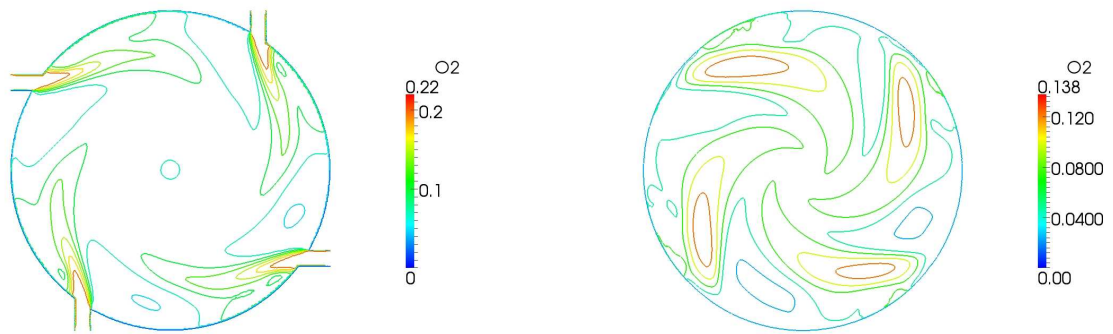


Figure 13: Oxygen flow field for 4 inlets configuration contour plot Figure 14: Oxygen flow field at the fuel grain for 4 inlets configuration contour plot

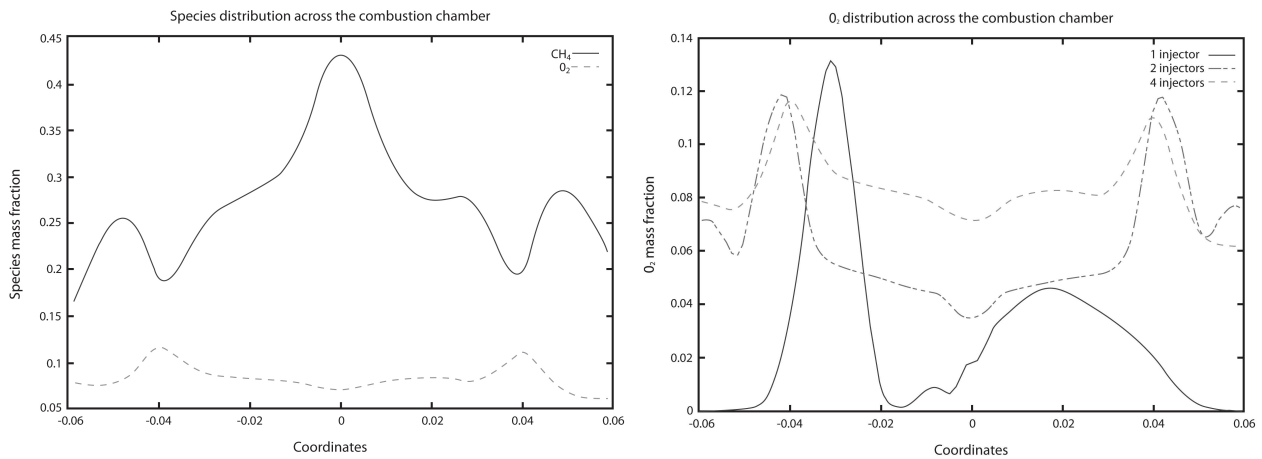


Figure 15: Species distribution across the combustion chamber for 2 Inlet configuration Figure 16: Oxygen distribution for different engine configurations

## 5. Pancake Hybrid Rocket Hot Flow Simulation

Although cold flow simulation is a useful tool to estimate the combustion chamber properties, the adequate results are not reachable until the full simulation with the reactions and correctly solved energy balance equation on the solid-fluid interface are computed. This problem was approached by the utilization of the code developed and presented in the benchmark case. Main simulation settings were kept in the original form as in benchmark case, including complex ignition system, turbulence model and chemical kinetics model (ref. table 4). The kinetics and boundary conditions of the flow are similar to the one used for cold flow simulation, with the intended difference in the fuel release kinetics velocity and the injector temperature.

Table 4: Hot flow simulation boundary conditions

Patch Name	$p$ [Pa]	$T$ [K]	$U$ [m/s]	$k$ [ $\frac{m^2}{s^2}$ ]
Inlet	$\frac{\partial p}{\partial x} = 0$	TV <sup>a</sup>	$10 \cdot \vec{n}$	0.01
Outlet	$10^6$	$\frac{\partial T}{\partial y} = 0$	$\frac{\partial \vec{U}}{\partial y} = 0$	$\frac{\partial k}{\partial y} = 0$
External Walls	$\frac{\partial p}{\partial x} = 0$	$\frac{\partial T}{\partial x} = 0$	$\vec{U} = 0$	$\frac{\partial k}{\partial x} = 0$
Fuel	$\frac{\partial p}{\partial y} = 0$	$\frac{\partial T}{\partial y} = 0$	Calculated	$\frac{\partial k}{\partial y} = 0$

<sup>a</sup>TV - Time variant

## NUMERICAL SIMULATION OF VORTEX COMBUSTION IN A HYBRID ROCKET MOTOR

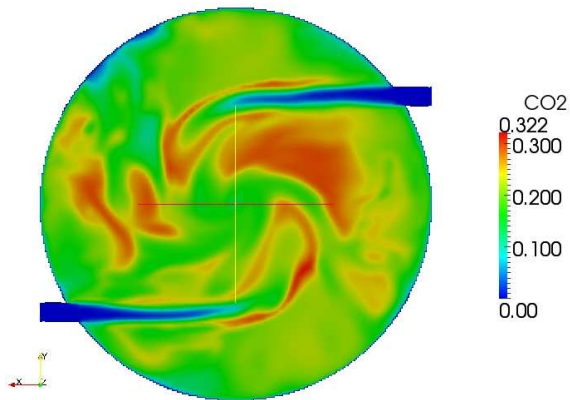
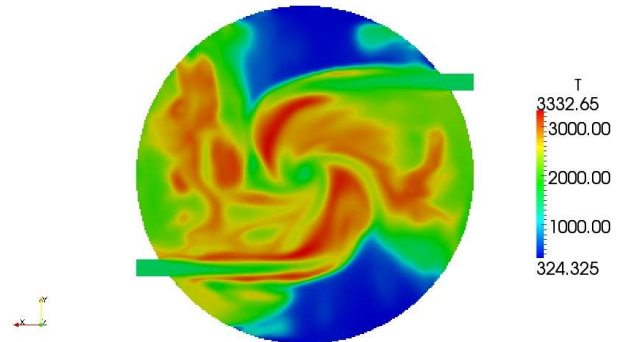
Figure 17:  $CO_2$  flow field

Figure 18: Temperature distribution [K]

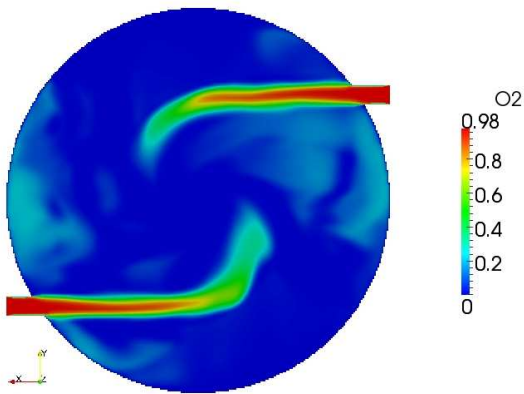
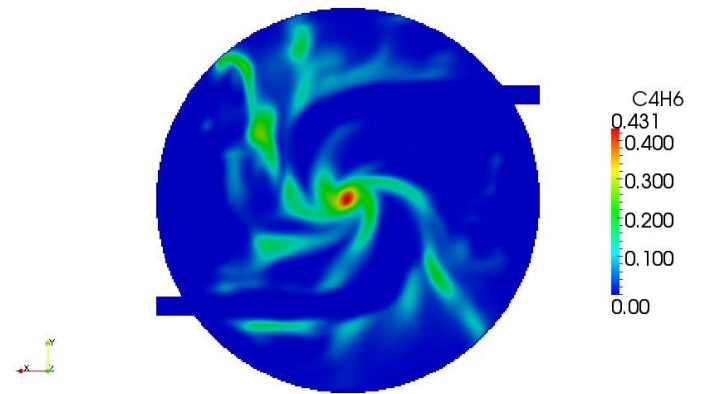
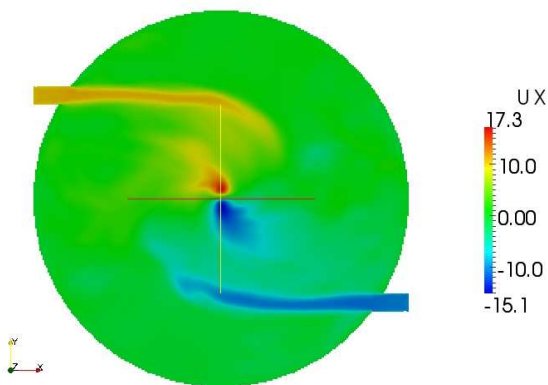
Figure 19:  $O_2$  flow fieldFigure 20:  $C_4H_6$  flow field

Figure 21: X velocity component flow field

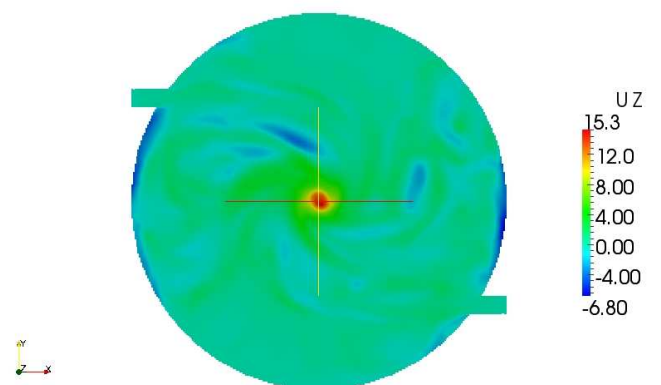


Figure 22: Z velocity component flow field

The results for 2 injectors configuration are analogous to the one from the cold flow simulation. When oxidizer is injected the reactive boundary layer is situated in close proximity to the fuel, and detaches downstream. Therefore, the regions with the high fuel emission zones will be situated close to the injectors. The center of the disk as it was observed by Rice<sup>10</sup> is a second emission area however no of circulation predicted by Chiaverini<sup>6</sup> was observed. Except of the regions close to the injected jets, where the fluctuation may cause downward movement, there is no evidence of

## NUMERICAL SIMULATION OF VORTEX COMBUSTION IN A HYBRID ROCKET MOTOR

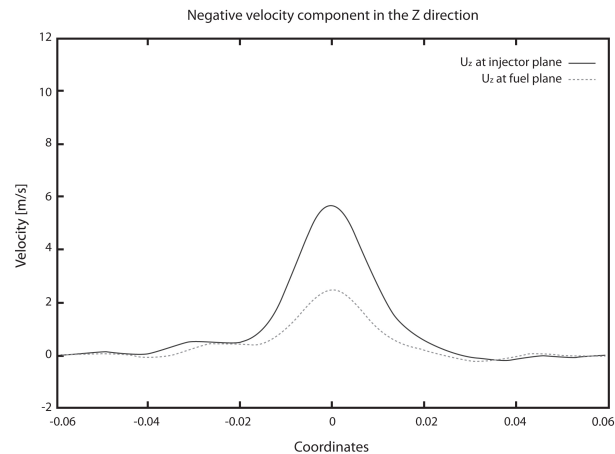


Figure 23: Z velocity component flow field for different cross-sections

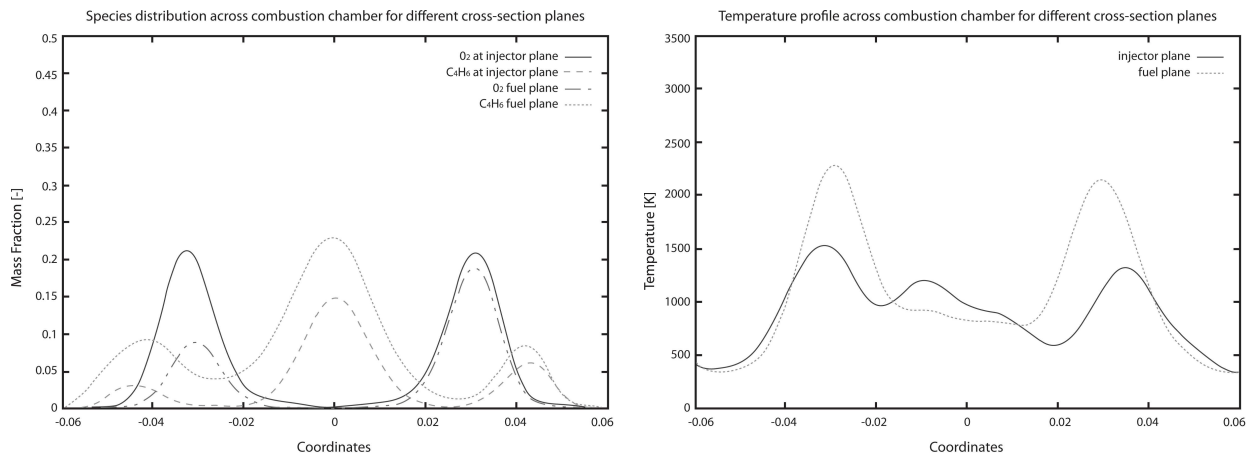


Figure 24: Species distribution across the combustion chamber for different cross-sections

Figure 25: Temperature distribution across the combustion chamber for different cross-sections

any other circulation tendency (Fig. 23). What can be however visible is the concentration of the unburnt fuel gases in the central part of the grain. Therefore this area works as an aft chamber mixing where additional reactions can take place between the oxygen and the unburnt fuel gases.

## 6. Conclusions

The work is the first comprehensive approach to the theoretical understanding of hybrid rocket engines in the pancake configuration using novel numerical tools. The turbulence model, based on large eddy simulation connected with the advanced multi-step chemical kinetics and radiation model (based on discrete ordinate method), gives better understanding of the processes taking place in the hybrid rocket engine combustion chamber. The benchmark 2-dimensional is used to verify a numerical model which afterwards is used for the construction of a 3-dimensional case based on VPH geometry. The cold flow parametric studies show that the number of injectors influences oxidizer distribution across the combustion chamber. For this reason a higher number of oxidizer injectors is preferable. High velocity of the injected oxidizer plays also an important role, not only thinning the boundary layer, which increases the fuel surface temperature, but also causes oxidizer jet cross-influence promoting oxidizer sweeping around the case. This in turn increase the oxidizer presence in the combustion chamber enhancing the combustion efficiency. The hot flow simulation gives additional information regarding species concentration and temperature distribution. The center part of the grain accumulates the fuel gases due to the inertia gained from the injected oxidizer. This part also is affected by the presence of non-reacted oxidizer, thus playing the role of aft-chamber. The energy released in this process causes additional fuel release from the central parts of the grain. However, the most intensive fuel release zones are located close to the injectors where the inflowing oxidizer promotes thin boundary layer.

## NUMERICAL SIMULATION OF VORTEX COMBUSTION IN A HYBRID ROCKET MOTOR

Future research should concentrate on the development of the tool that could cover effects present on the surface of the grain which influence the intensity of the mass release and the oxidizer-to-fuel shifts (ditching effect). Future simulation should bound the scale of the combustion chamber diameter with the fuel mass release coefficients. This tool would be valuable for the precise engine performance estimation.

## Nomenclature

$Le = \frac{\alpha}{D}$	Lewis Number	$a$	The number of angels per unit area
$\alpha_t$	turbulent thermal diffusion	$b$	temperature exponent
$\bar{\omega}$	Chemical source term	$D_t$	turbulent mass diffusion
$\delta\tau$	residence time	$E_a$	activation energy
$\delta_{ij}$	The Dirac delta	$h_t$	total enthalpy, $\frac{J}{kg}$
$\nu_t$	turbulent viscosity	$I(\vec{s})$	radiation intensity
$\Psi(\vec{s}^i, \vec{s}^j)$	phase scattering function	$k$	absorbtion coefficient
$\rho$	density, $\frac{kg}{m^3}$	$N_r$	number of reactants
$\sigma_s$	scattering coefficient	$Pr = \frac{\nu}{\alpha}$	Prandtl Number
$\tau_c$	chemical time	$R_k$	reaction rate
$\tau_{ij}^R$	The Reynolds stress tensor	$t$	time, <i>sec</i>
$\tau_{mix}$	turbulent mixing time	$Y_k$	mass ratio
$A$	pre-exponentiation coefficient		

## References

- [1] *OpenFOAM, The Open Source CFD Toolbox : User Guide*, 2014.
- [2] Ganu A., Mor M., and Goldman C. Analysis and characteristics of choked swirling nozzle flows. *AIAA Journal*, 43(10):2177–2181, 2005.
- [3] Mazzetti A., Merotto L., and Pinarello G. Paraffin-based hybrid rocket engines applications: A review and a market perspective. *Acta Astronautica*, 126:286–297, 2016.
- [4] Mazzettii A. *Numerical Modeling and Simulation of Combustion Processes in Hybrid Rocket Engines*. PhD thesis, Politecnico di Milano, 2014.
- [5] Paravan C., Glowacki J., Carlotti S., Maggi F., and Galfetti L. Vortex combustion in a hybrid rocket motor. In *52nd AIAA/SAE/ASEE Joint Propulsion Conference*, 2016.
- [6] Kuo K.K. Chiaverini M.J. *Fundamentals of Hybrid Rocket Combustion and Propulsion*, volume 218. Progress in Astronautics and Aeronautics, Arlington,USA, 2007.
- [7] Lin C.L. and Chiu H.H. Numerical analysis of spray combustion in hybrid rockets. In *31th AIAA-95-2687*, San Diego, CA USA, 1995. 63-505.
- [8] Sirignano W. Coronetti A. Numerical analysis of hybrid rocket combustion. *Journal of Propulsion and Power*, 29(2), 2013.
- [9] Gibbon D.M., Haag G., Lin S., and Kwok C.K. *Invastigation of an Alternative Geometry Hybrid Rocket for Small Spacecraft Orbit Transfer*. DTIC Technical Report, 2001. AD No. 393398.
- [10] Rice E.E., Gramer D.J., St. Clair C.P., and Chiaverini M.J. Mars isru  $co/o_2$  rocket engine development and testing. In *7th NASA International Microgravity Combustion Symposium*, 2003.

## NUMERICAL SIMULATION OF VORTEX COMBUSTION IN A HYBRID ROCKET MOTOR

- [11] Cheng G., Farmer R., Jones H., and McFarlane J. Numerical simulation of the internal ballistics of a hybrid rocket motor. In *Aerospace Sciences Meeting and Exhibit*, 1994. 63-505.
- [12] Gariani G., Maggi F., and Galfetti L. Simulation code for hybrid rocket combustion. In *46th AIAA/ASME/SAE/ASEE Joint Propulsion Conference and Exhibit*, Nashville, TN, 2010. 2010-6872.
- [13] Gariani G., Maggi F., and Galfetti L. Numerical simulation of htpb combustion in a 2d hybrid slab combustor. *Acta Astronautica*, 69:289–296, 2011.
- [14] Haag G. *Alternative Geometry Hybrid Rockets For Spacecraft Orbit Transfer*. PhD thesis, University of Surrey, 2001.
- [15] Haag G., Sweeting M., and Richardson G. An alternative geometry hybrid rocket for spacecraft orbit transfer manoeuvres. In *51st International Astronautical Congress*, 2000. IAF Paper 00-W.2.07.
- [16] Risha G.A., Harting K.K., and Peretz D.E. and Joch H.S. Kuo A. Pyrolysis and combustion of solid fuels in various oxidizing environments. In *34th AIAA/ASME/SAE/ASEE Joint Propulsion Conference and Exhibit*, Cleveland, OH, USA, 1998. 3184.
- [17] Weller H.G., Tabor G., Jasak H., and Fureby C. A tensorial approach to computational continuum mechanics using object-oriented techniques. *COMPUTERS IN PHYSICS*, 12(6), 1998.
- [18] Glowacki J. *Hybrid Rocket for in-space propulsion*. PhD thesis, Politecnico di Milano, 2016.
- [19] W. J. Knuth, D. J. Gramer, M. J. Chiaverini, Sauer, Whitesands J. A., R. H., , and Dill R. A. Preliminary cfd analysis of the vortex hybrid rocket chamber and nozzle flowfield. In *AIAA/SAE/ASME/ASEE 34th Joint Propulsion Conference and Exhibit*, Cleveland, OH, 1998. AIAA Paper 98-3351.
- [20] Gilbert M. Marxman G. Turbulent boundary combustion in the hybrid rocket. In *9th International Combustion Symposium*, 1963.
- [21] Muzzy R.J. Marxman G., Wooldridge M. Fundamentals of hybrid boundary layer combustion. In *AIAA Heterogeneous Combustion Conference*, Palm Beach, FL, USA, 1963. 63-505.
- [22] Smoot L.D. Price C.F. Regression rate mechanism of nonmetalized hybrid rocket systems. In *2nd Aerospace Science Meeting*, New York, NY, USA, 1965. 371-383.
- [23] Gordon S. and McBride B.J. *Development of Universal Model of Turbulent Spray Combustion, TFR Research Proposal*. Chalmers University of Technology, 2001.
- [24] V. Sankaran and C. L. Merkle. Size scale-up in hybrid rocket motors. In *34th Aerospace Sciences Meeting and Exhibit*, Reno, NV, Jan. 1996., 1996. 96-0647.
- [25] N. Serin and Y. A. Gogus. Navier stokes investigation on reacting flowfield of htpb o2 hybrid motor and regression rate evaluation. In *AIAA/SAE/ASME/ASEE 39th Joint Propulsion Conference and Exhibit*, Huntsville, AL, USA, 2003. 4462.
- [26] S. Yuasa, Shimada O., T. Imamura, Tamura, T., and K. Yamamoto. A technique for improving the performance of hybrid rocket engines. *AIAA*, 99:2322, 1999.